RESEARCH ARTICLE

BON VIEW PUBLISHING

An Innovative Measurement Protocol for Determining the True Glass Transition Temperature of Chalcogenide Glasses by Differential Scanning Calorimetry

Thomas J. Loretz[1,*] , **Rashi Sharma**[2] , **Anna Zachariou**[2], **Richard A. Loretz**[3] , **Myungkoo Kang**[4] and **Kathleen A. Richardson**[2]

[1]*Computer Engineering Service, USA*

[2]*College of Optics and Photonics, University of Central Florida, USA*

[3]*Nuclear Physics Consultant, USA*

[4]*NYS College of Ceramics, Alfred University, USA*

Abstract: The glass transition temperature, T_g, is one of the most important physical attributes of a glass. The value of T_g often defines how a glass is made and used and dramatically impacts the electrical, mechanical, optical, and transport properties of the material. Despite its importance, the manner in which the thermal equilibrium temperature value for T_g is defined and measured in the chalcogenide glass community varies widely among researchers and practitioners leading to confusion about the term and misrepresentation of the property. Unique to this glass community, the measurement instrument of choice is the Differential Scanning Calorimeter (DSC). Countless variations in practice, coupled with incorrect equations which have been passed down unchallenged for more than 55 years, have yielded hundreds of peer-reviewed research papers and dozens of undergraduate and graduate theses. We review representative research and apply equations recently corrected by members of our team to reveal how a novel mathematical extrapolation technique to a "zero" heating rate limit provides an innovative analytical technique which will determine what we call the "true" glass transition temperature $T_g(0)$ of a chalcogenide glass composition at isothermal equilibrium.

Keywords: glass transition temperature, chalcogenide glass, DSC, zero heating rate analysis

1. Introduction

1.1. Glass transition theory for amorphous materials

The glass transition temperature is a unique property, positioned more-or-less in the middle of a narrow temperature range window (*sometimes referred to as the glass transition region*). Originally theorized for and applied to oxide glasses, it defines the isothermal equilibrium temperature at which a well-homogenized and well-annealed glass can no longer be deemed a rigid, elastic material, nor a viscous, inelastic material [1]. Arguably, therefore, when properly measured, such a definition makes the glass transition temperature (T_g) a material "constant" for oxide glasses. Moreover, when considering only the isothermal equilibrium state, its value should be independent of the direction of approach and independent of the rate of approach used to reach thermal equilibrium, thereby justifying our decision to dismiss theories

and concerns associated with a hypothetical "*fictive temperature*" which may have influenced results for glasses studied.

Since a "window" of temperatures is involved, the glass transition temperature has always been best defined as the specific temperature at which this well-homogenized and well-annealed amorphous material achieves a characteristic viscosity, whereby molecular relaxation occurs at a rate which removes all internal **strain** in a specific time period, which is ultimately determined by the molecular "makeup" of the glass. The glass transition temperature's defining time period for relaxation will be shown to be typically short and on the order of 100 s at isothermal mass. This means that the exact **viscosity value** associated with the isothermal equilibrium glass transition temperature (*henceforth*, T_g or what we have elected to call $T_g(0)$ or the true T_g) is dictated by the type of amorphous material being evaluated (*e.g., chalcogenide, oxide, halide, oxyhalide, polymer, etc.,*). Hence, the true T_g is a defined material property and determined by an isothermal viscosity. More importantly, it is a singular property for all glasses and "glass-like" amorphous materials, including polymers. Any attempts to assign additional isothermal equilibrium glass transitions beyond the first assignment ignore this explicit singularity rule.

Corresponding author: Thomas J. Loretz, Computer Engineering Service, USA. Email: tom@CESWorldHQ.com

This paper focuses on chalcogenide glasses (ChGs), amorphous materials which contain neither oxygen nor any other anion beyond those found resident in Group VI and other heavier elements of the periodic table. We focus on ChGs because we recognize that great confusion exists within this specialized glass community concerning the definition, significance, and measurement of the isothermal equilibrium glass transition temperature. While ChGs are utilized for the purpose of example for this study, we contend that the premises and analytical strategies discussed are applicable to virtually all other amorphous materials. ChGs are not ionically bonded materials like oxide, halide, or oxyhalide glasses. Rather, structurally, their molecular units are bonded by van der Waals forces and covalency, with the weaker, vdW bonds securing the predominant percentage for compositions in most families [2]. They are most commonly made by melting specific family elements, followed by rapid quenching which freezes the molecular melts to an amorphous state.

This paper presents a new approach to explain why previous methods used by ChG researchers and practitioners introduce misrepresentations and inaccuracies for reported values of T_g, especially evident when employing high heating rates in Differential Scanning Calorimeter (DSC) evaluations. Our literature review shows that DSC measurement determinations of T_g are most commonly made by using a fixed heating rate of 10 K/min (*aka:10 °C/min*)[1]. We will explain and demonstrate why this heating rate by itself does not yield an accurate value for the isothermal equilibrium glass transition. We will propose a new theory and analytical strategy which demonstrates that the correct determination of T_g requires multiple heating rates and mathematical extrapolation to a "zero" heating rate (ZHR) limit [3]. Through our analysis, we conclusively illustrate how this approach aligns with viscometric data yielding a more representative value as a material property.

1.2. Utilizing thermal analysis tools to quantify the true T_g

Prior to presenting the revised approach to quantify T_g for ChGs and other glass materials, we review methodology that is most regularly used by our community and its shortcomings. This paper presents a measurement protocol and the results of glass transition temperature research performed on a variety of ChGs, representing several different compositional families. We highlight studies using viscometry, dilatometry, and differential scanning calorimetry measurement techniques as a source of data for comparison and analysis. Important to the presentation of these data, the often unreported variables of material and measurements and their sources have been clearly defined and are highlighted to the reader.

As previously discussed, the temperature and viscosity values associated with the T_g for a given composition are molecular network-dependent. For all glasses, T_g exists in a physically small temperature range. It correlates with structural metamorphosis of a mass at isothermal, equilibrium state, transitioning from an elastic to an inelastic material domain. With such definition, DSC-derived T_g values for ChGs cannot be "variables" relying on *(undefined)* sample mass, sample annual quality, sample environment, and most critically, sample heating rate as they are represented in countless studies found in literature. Consequently, miscalculations typically made in the DSC measurement of T_g (*and by extension, other endothermic and exothermic values*) are directly related to inappropriate measurement protocols, which lack needed specificity to result in consistency and low error. For

example, faster heating rates, larger sample masses, the absence of a suitable reference cell material, and the use of quenched, non-annealed samples all contribute to higher *pseudo-T_g temperatures* being reported. Hence, without attention to the quantification and reporting of these details, comparison across researchers for the "same" composition is difficult to achieve.

As many of these instrument variables are not considered and, in most cases, not reported in studies, published DSC data continue to be made at high heating rates, and the critical upper use temperature of a glass (*located slightly below the strain point temperature and associated strain point viscosity*) is often as a result, substantially overstated. These errors in T_g temperature determination have led to electrical, mechanical, and optical problems for glasses used at elevated temperatures and have caused field application issues, including anti-reflection coating failure, unwanted nuclei production, excessive optical absorbance, lens design performance failure, component storage-related failures and in the case of C-RAMs (*Phase Change Memory*), inaccurate calculations leading to thermal runaway. Hence, for accurate glass performance behavior prediction, a *singular* and *accurate* T_g value is essential. The analysis in this study aims to define and quantify these variables and methods.

1.2.1. Molecular relaxation

A vast number of liquids can be made into amorphous materials at room temperature by rapidly cooling them at a rate whereby crystallization is avoided, and the melt enters the so-called "supercooled phase".

From classical Newtonian fluid physics, the dynamic viscosity is defined as:

$$\eta = \frac{\frac{F}{A}}{\frac{\partial v}{\partial x}} \tag{1}$$

where: $\boldsymbol{\eta}$ is the dynamic viscosity with units of *Pascal Seconds (Pa.s)*, $\boldsymbol{F}$ is the Shear Force applied per unit area, $\mathbf{A}$, and $\partial \mathbf{v}/\partial \mathbf{x}$ is the velocity gradient of shear [4]. Beyond dynamic viscosity data, Equation (1) provides a simple means to define the molecular relaxation time constant associated with the glass viscosity. Berthier and Biroli investigated the physics of molecular and polymeric glasses at their melting temperatures from the standpoint of molecular bonding behavior and density fluctuation relaxation [5]. In their work, they developed a theoretical model which related an amorphous liquid's molecular radius and molecular mass at its effective melt temperature by unifying the energy and temperature on the same scale, through a novel application of the Boltzmann constant. Using their model's equation, they approximate the molecular relaxation time to be about 1 to 3 picoseconds (ps) for the vast number of glasses within this class of materials.

1.2.2. Viscosity

Figure 1 provides the viscosity profile for the Vogel-Tammann-Fulcher (VFT) equation for an Arsenic-Selenium-Sulfide composition made in the University of Central Florida (UCF) laboratory, using previously reported melt-quench protocols employed for exploratory glass melts where optical quality (high optical refractive index homogeneity) had yet to be optimized [6]. To compile the data illustrated in Figure 1, various viscosity measurement techniques and data points were employed, including the dilatometric softening point, beam-bending values, and high-temperature viscometry values. The applicable VFT equation is derived from the Bond Strength–Coordination Number-Fluctuation (BSCNF) model. (Equation (2)). The BSCNF model explains viscous flow as a breaking and/or twisting of the bonds that connect the melt's structural units [7].

---

[1]Throughout this paper, the terms K/min and °C/min are applied interchangeably as an equation or discussion may require.

Figure 1
Viscosity temperature profile for an As-Se-S chalcogenide glass composition
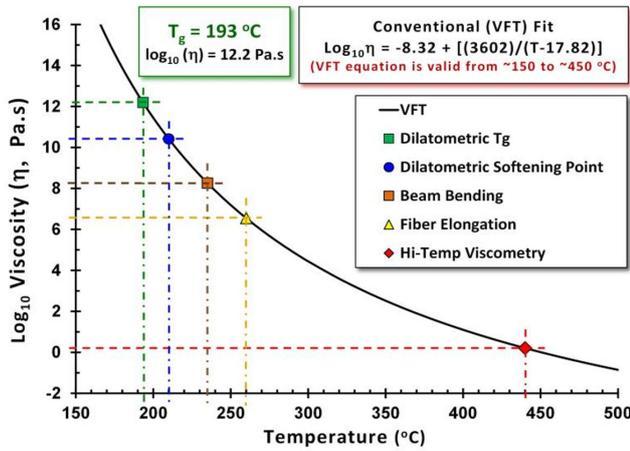
This reduces to the equation:

$$\log_{10}(\eta) = A + B/(T - T_0) \qquad (3)$$

The constants A, B, and T_0 in Equation (3) are solved with matrix algebra in the normal manner, using three equations with three unknowns. Dilatometric softening point (T_D), beam-bending data, and high-temperature viscometry data were used to achieve this separation between viscosity points. The less accurate T_D data were also replaced with fiber elongation viscosity data. This approach provided good VFT viscosity modeling results for the viscosity range, restricted to between 1e+02 Pa.s and 1e+15 Pa.s.

1.3. Differential Scanning Calorimetry (DSC)

A review of the past and current research (*as reported in the references used to collate data for this study*) indicates that the critical thermal properties of ChGs are most often evaluated using DSC analysis. Reasons for this equipment choice are predominantly associated with (1) the speed of measurement, (2) the potential for highly accurate and useful data, and (3) the small sample mass required. More significantly, due to extreme material and fabrication equipment costs, typical research laboratory ChG melts rarely exceed 50 grams and prohibit fabrication of useful samples for dilatometry and most viscometry measurements.

Over the years, various methods have been developed for DSC instruments. In the 1990s, a modified instrument was developed to include heat capacity measurement capabilities, further expanding the capabilities of DSC. Other tools and method changes have been explored including heating the glass from room temperature to a higher temperature at a fixed heating rate (*non-isothermal technique*), introducing the glass to a furnace at a fixed temperature (*isothermal technique*), and modulating a linear heating rate, sinusoidally (*aka: Modulated Differential Scanning Calorimetry, MDSC*) [8–11].

For more than 55 years, an abundance of literature supplies evidence that glasses in general, and ChGs in particular, have been studied using a DSC linear heating ramp rate approach (*non-isothermal*). Here, a power

versus temperature thermogram is produced as a visual means to interpret the data generated. The heat flow rates ($\partial H/\partial t$) or ($\partial H/\partial T$) report the summation of all power being generated at a point in time or temperature, respectively. DSC heating rates vary for the most part, between 5 and 60 K/min. The most often used rates seem to be 10 and 20 K/min, with 10 K/min being the preferred. For the most part, little or no discussion is often provided to explain a researcher's choice of heating rate protocol, sample preparation, instrument parameters, and sample mass used. The absence of these experimental details creates a challenge for other researchers who wish to duplicate the work [12–15].

DSC data have been used to determine the glass transition temperature, the endothermic and exothermic activity (*enthalpy behavior*) of a glass, the crystallization temperature (T_x), and "*a melting temperature*" (T_m). DSC measurements of these reference temperatures have contributed to the understanding of a glass' crystallization stability or, in the case of phase change media, crystallization susceptibility. Researchers have employed the "Moynihan method" (*developed in the 1970s*) to process DSC-derived thermogram data with a goal to determine the activation energy for structural relaxation [16–23]. We will provide further information about this method, shortly. Although modern DSC instruments supply a special crucible sensor package and software for a differential reference cell measurement, a carefully chosen reference sample powder is rarely used, leaving the differential "reference" material to be DSC furnace environmental atmosphere. We believe this to be a source of experimental error. As will be discussed below, we will demonstrate how a carefully selected reference powder, in combination with a mathematical technique, can be used to establish a ***zero enthalpy*** thermogram baseline with a concurrent enhancement to thermogram sensitivity and definition at all ramp rates.

Equations have been developed by Ozawa, Kissinger, and others to apply DSC data to estimate the activation energy for crystallization and to gain insight to the "bonding energy" for a particular glassy system [24–29]. Members of our team published a research article which reviewed these equations. Their study addressed specific problems with these crystallization equations, provided corrected equations for future use, and demonstrated the application of the new equations using a recently developed ChG family [30]. Beyond this work, researchers have contributed to our understanding of DSC and ChG material analysis in other areas [31–35].

As will be shown, accurate determination of T_g is related to a DSC measurement that is conducted in the limit of a ZHR so that the measurement provides results indicative of the isothermal mass, fully-relaxed, equilibrium network. In a review of Moynihan's work, our team members showed that he correlated DSC thermogram data with sample heating rate in an attempt to apply an Arrhenius template and derive what he called an activation energy of transition (*arguably, an activation energy of thermal event data*) [3]. Examining his analysis in detail, our team members concluded that Moynihan may not have recognized that the thermogram data offered a clear path to a unique T_g at the stable equilibrium state for any given composition. They have identified and illustrated the challenges associated with both the Moynihan and Kissinger models and have taken the initiative to correct these researcher's equations. Additionally, they have provided a conversion equation which relates activation energy values for the two models. They have effectively demonstrated how their modified equations can be applied to glasses in general and, more specifically, to ChGs, to provide an accurate determination of the isothermal mass, equilibrium T_g. Finally, to extend the understanding realized by the above corrections to the legacy approach originally proposed by Moynihan, they developed a mathematical model which applies DSC thermogram data effectively to determine this *true glass transition temperature*, ($T_g(0)$).

Their model is:

$$\mathbf{T_g(0)} = \mathbf{T_{g\ (measured)}}(\boldsymbol{\alpha}) - \mathbf{C\ ln}(1 + \boldsymbol{\alpha}/\boldsymbol{\alpha_1}) \tag{7}$$

where: $\mathbf{T_{g\ (measured)}}(\boldsymbol{\alpha})$ is the $\boldsymbol{T_g}$ inferred from DSC measurements at an $\boldsymbol{\alpha}$ heating rate,

$\mathbf{T_g(0)}$ is the limiting $\boldsymbol{T_g}$ as the DSC heating rate approaches zero,

$\boldsymbol{C}$ is a constant (K degrees) equal to the slope of $\mathbf{T_g}$ vs. $\boldsymbol{ln}(1 + \boldsymbol{\alpha}/\boldsymbol{\alpha_1})$,

$\boldsymbol{\alpha}$ is the heating rate (*K/min or K/sec or K/hr*) and

$\boldsymbol{\alpha_1} = 1\ K/\min,\ (1/60)\ K/\sec or\ 60\ K/hr$, respectively.

Note the logarithmic nature of the model and the requirement to solve for the glass composition's constant "$\boldsymbol{C}$" value (*slope of the line*). Two properly chosen heating rates (*such as 1 K/min and 10 K/min*), coupled with care in sample preparation, equipment normalization, and other critical factors (*which we will describe below*), will yield a solution for **C** and a reasonable value for $\mathbf{T_g(0)}$, the glass transition temperature at a ZHR, which our laboratory work has shown to be typically within ±2 °C of values determined by independent methods. When more accurate and reliable results are required, we recommend a minimum of three-3 experimental heating rates, having reasonable mathematical separation to account for experimental error (*such as 2, 5, and 10 K/min or 3, 10, and 20 K/min*). It is also important to exercise reasonable care in sample preparation and transfer, as masses are quite small.

The following sections describe the details necessary to apply our measurement methodology to obtain high accuracy and true *Tg* values. This protocol, when applied in practice, helps to mitigate most of the challenges observed by researchers when trying to generate reproducible data, when compared across research teams and alternate measurement protocols. For the purpose of illustration in this paper, our method is applied to a range of ChG families, and parallel, independent measurement techniques are utilized to validate our claims, thus solidifying our conclusions.

2. Experimental: New DSC Method Details

Experimental determination of key thermal properties of glasses can be realized by a variety of thermal analysis methods including dilatometry, differential scanning calorimetry, and the previously described viscometry evaluation. Here we present a new means for quantifying a glass' accurate isothermal mass, equilibrium *Tg*. We provide a detailed explanation of sample preparation, sample form, and measurement protocol, which together provide for a complete comparison of data realized by these fundamental techniques.

2.1. Melt preparation

Five commercial and two laboratory-scale ChGs were used in this study. One of the experimental glasses was transitioned for scale-up from the university laboratory and melted by a well-known, commercial infrared optical quality glass manufacturer [36]. For this large mass melt (>2 Kg), advanced and proprietary fabrication techniques were employed which were designed to eliminate the introduction of all unwanted nuclei and to yield a glass of exceptional optical homogeneity. The other experimental glass was prepared in the Glass Processing and Characterization Laboratory (GPCL) at UCF in a fused silica ampoule, via melt-quenching techniques using previously reported protocols [6]. All "lab-scale" and commercial melts were made with 5N's purity or better elemental starting materials.

Table 1
Chalcogenide glass compositions studied

Glass Name	ChG Family	Unique attributes or features
AMTIR-1	Ge-As-Se	Commercial melt, multi-Kg volumes per year
AMTIR-2	As-Se	Commercial melt, multi-Kg volumes per year
AMTIR-3	Ge-Sb-Se	Commercial melt, multi-Kg volumes per year
AMTIR-6	As-S	Commercial melt, multi-Kg volumes per year
AMTIR-F1	As-Se-Te	Commercial melt, several Kg volumes per year
18-UCF-6	Ge-As-Pb-Se	Exploratory composition, Commercial melt
UCF-512	Ge-As-Se	Lab-scale melt, Pb-free version of 18-UCF-6

The five commercial ChGs were as follows: AMTIR-1, AMTIR-2, AMTIR-3, AMTIR-6, and AMTIR-F1 (*a Germanium-Arsenic-Selenide, an Arsenic-Selenide, a Germanium-Antimony-Selenide, an Arsenic-Sulfide, and an Arsenic-Selenium-Telluride glass, respectively*). The experimental laboratory composition prepared using commercial equipment and techniques was a 5.0 atomic percent lead (Pb) containing Germanium-Arsenic-Selenide composition (18-UCF-6). The other glass was the Pb-free, base glass composition (UCF-512), prepared in UCF's GPCL.

Table 1 summarizes these ChG compositions by name, basic elemental makeup and any unique features and/or attributes which may be useful in understanding how they differ from each other. Actual elemental composition and specific melting methods are not provided, as this information is considered proprietary in nature.

2.2. Sample preparation: Dilatometry analysis

All glass sample dimensions used for dilatometric measurements were approximately 3.5 mm in diameter and 50 mm in length. Keeping the diameter as small as practical, reduces sample mass and aids in reducing thermal conductivity-related issues. The samples were heated at a rate of 0.5 K/min, with a 2.5 g Linear Variable Differential Transformer (LVDT) sensor load applied. A computer-controlled, horizontal furnace dilatometer was employed (*designed and built by Computer Engineering Service and calibrated with NIST standards*). During measurement, temperatures and displacement data are transferred electronically from a Keysight Model 34970A datalogger to an EXCEL® spreadsheet for analysis and graphical interchange. The quartz holder of this laboratory dilatometer accepts glass rods, 3 to 5 mm in diameter, 50.0 ± 0.5 mm long (*measured to 0.05 mm for CTE calculation purposes*) with a dome-radius at each end for better pushrod contact. A *LVDT* is attached to an adjustable tension, dual beryllium-copper spring mount which applies an initial sample load of 2.5 ± 0.5 grams, via a fused silica pushrod. Dual Be-Cu springs permit extremely low contact forces to be applied and yield excellent sample measurement precision. For our dilatometer, we have determined that our protocol yields a Dilatometric Softening Point temperature, T_D value, for ChGs which typically correlates to a viscosity value between $\log_{10}(\eta) = 10.2$ and 10.6 Pa.s. Researchers are encouraged to calibrate their own instruments, as required.

2.3. Sample preparation: DSC analysis

UCF used a Netzsch 204F1 Phoenix model DSC with elemental aluminum crucibles for all measurements made in this study. Aluminum was chosen because it is inexpensive, readily available, maintains its high-temperature strength in thin gauges, and has very high thermal conductivity. To enable a systematic comparison of data in our study, all glasses were annealed, then crushed and sieved to pass through a standard ASTM 200-mesh sieve (< 75-micron particle size). This particle size represents a good balance between thermal properties and ease of fabrication. Sample annealing ensures that the primary endotherm's behavior is appropriately influenced by molecular relaxation at high heating rates. The small thermal conductivity values for ChGs ($\sim$0.01 cal/sec.cm.$^{\circ}$C) necessitate a stable, compatible reference crucible material to: (a) establish a useful "zero-power" output level, (b) improve the differential contrast in areas of enthalpic activity, (c) provide stability for low output signals, (d) enhance peak definition, and (e) improve the performance of a simple mathematical technique to correct the thermogram baseline. The use of these criteria is supported by our experiments and detailed analysis of measurement outcomes.

Based on a recommendation from CES, yellow lead oxide, the orthorhombic form of the material (β-PbO), was used as a reference standard. This was done to assess the quality of an "air-referenced" thermogram analysis, a protocol which has been commonly used in all research papers referenced to date. This material was chosen because of its comparable thermal conductivity to ChG ($\sim$0.03 cal/sec.cm.$^{\circ}$C), its ability to be easily sieved to a comparable mass as the glass sample, and its absence of any enthalpic behavior below 400 $^{\circ}$C. Therefore, unlike an air reference (*or any other DSC purging gas atmosphere*), PbO has the ability to enhance signal-to-noise ratio, improve thermogram definition, and reduce the overall signal distortion at both low and high heating rates. Several preliminary experiments were made on various ChGs with and without PbO in our aluminum reference crucibles.

Similar in scope to the PbO experiments, several preliminary experiments were made to assess the influence of sample mass and reference mass size on DSC thermal run data. In some experiments, 40 mg sample masses were accompanied by 20 mg PbO references. The results show that the differences in resolution and total enthalpy were small when PbO was used as a reference. All DSC crucibles were high-purity aluminum.

Ultimately, a standard sample mass of 20 mg ($\pm$ 1 mg) and a standard PbO reference mass of 20 mg ($\pm$ 1 mg) were used. These values were found to provide the best trade-off between low-level output of low-noise data at reduced heating rates and enhanced peak definition for increased heating rates. This trade-off was especially important as it ensured the generation of well-behaved output data for the heating rate-derived, glass transition area, thus permitting easy interpretation of the curve's first derivatives.

For ChGs, it was determined that the glass sample and the reference powder should be soaked in their DSC crucibles at about 40 $^{\circ}$C below the **strain point temperature** of the glass composition for 15 minutes, prior to applying a chosen positive heating ramp. Beyond eliminating wasted measurement time, applying this method to an annealed glass positions the material to relax properly at any heating rate, fast or slow once the strain point is reached. Thus, this technique pre-heats the exceptionally low thermal conductivity glass powder sufficiently to reduce thermal inertia and associated lag normally found in DSC data produced on unannealed or "under-annealed" material. It also vastly improves the quality of the thermogram generated in the immediate area of the glass transition.

To determine a sample's strain point temperature, we recommend measuring the glass' thermal expansion behavior first, using the above-described protocol. Alternately, one may run a 3 K/min, uncorrected DSC "quick test" from room temperature to just past the material's first endotherm (*a feature present with all glasses and associated solely with molecular relaxation*). For a reasonable starting value for most ChGs, subtract 45 °C from the temperature of the Full Width Half Maximum "leading edge" (*FWHM le*) of this first endotherm profile. (In a future article, slated for 2025, members of our team will explain how strain point, annealing point, and glass transition "endpoint" temperatures can be determined very accurately from DSC thermogram experiments using techniques similar to those explained herein.)

## 3. Results and Discussion: DSC Determination of T_g: (Example Using AMTIR-1 ChG)

AMTIR-1 is the first of seven significantly different ChGs to have its T_g determined for this paper, using our new method. AMTIR-1 is a Ge_{33}-As_{12}-Se_{55}, general purpose infrared optical glass used for commercial and defense applications. It exhibits particularly good strength behavior and devitrification resistance, under all types of thermal cycling. Detailed instructions will be provided for each step in the T_g determination process for AMTIR-1, by way of graphical illustration and explanation. These data are illustrated step-wise, in Figure 2. All other glass types will be treated in the identical manner and only final data results will be presented for them.

In keeping with the tenets of our Equation (7) found above and the mathematical corrections previously discussed [3], the experimental data for all ChGs in this study were generated from 10 K/min and 1 K/min DSC experiments. This offered a useful 10:1 ratio for use with our model and more importantly provided data values close to the "zero-limit" heating rate.

For most glasses, the enthalpy found immediately after the first endotherm should be at baseline level. (An exception exists for certain crystallizable glasses which may have a nucleation endotherm near or integrated within this first endotherm, depending upon the heating rate.) Due to equipment and sample preparation issues, an uncorrected (*pre-normalization or baseline correction*) thermogram rarely portrays this reality accurately. To achieve accurate determination of present and future key thermal points and, more importantly, accurate enthalpy values, a method to establish a baseline correction was developed. This method requires (1) locating a reasonable zone of known "zero" enthalpy behavior beyond the first endotherm (*alternately, immediately after the right, higher temperature side of the second exotherm, if present and if this is the endotherm of interest*), (2) selecting two temperatures and their associated raw enthalpy data points on either end of this zone with a separation of at least 35 °C (*empirically determined value, useful for most ChGs*), (3) applying an EXCEL trendline feature to determine the linear regression equation which satisfies the straight line fit between these points, and (4) subtracting the solution of this equation from the corresponding raw enthalpy data values for each temperature in the data series.

This procedure creates a new column of DSC enthalpy data, with the instrument's typical default units of mw/mg. This new series is plotted against the corresponding temperature points and a normalized curve set is generated. This baseline correction procedure was applied to all experimental data presented herein, along with trendline and corresponding regression equations. The temperatures of 415 °C and 450 °C were selected for the "trendline" limits. Choosing the regression line limits in this manner is the key to baseline correction success for any ChG,

Figure 2
Raw 10 K/min DSC data for AMTIR-1 with linear regression equation, (b) Normalized 10 K/min DSC data for AMTIR-1 with $T_g(\alpha)$ and $T_D(\alpha)$ key points identified, where $\alpha = 10$. (See Table 2 for usage), (c) Raw 1 K/min DSC data for AMTIR-1 with EXCEL regression equation, (d) Normalized 1 K/min DSC data for AMTIR-1 with $T_g(\alpha)$ and $T_D(\alpha)$ key points identified, where $\alpha = 1$. (See Table 2 for usage), (e) Figure 2(b) converted to proper DCS enthalpy units of J/mol.s., (f) Figure 2(d) converted to proper DSC enthalpy units of J/mol.s
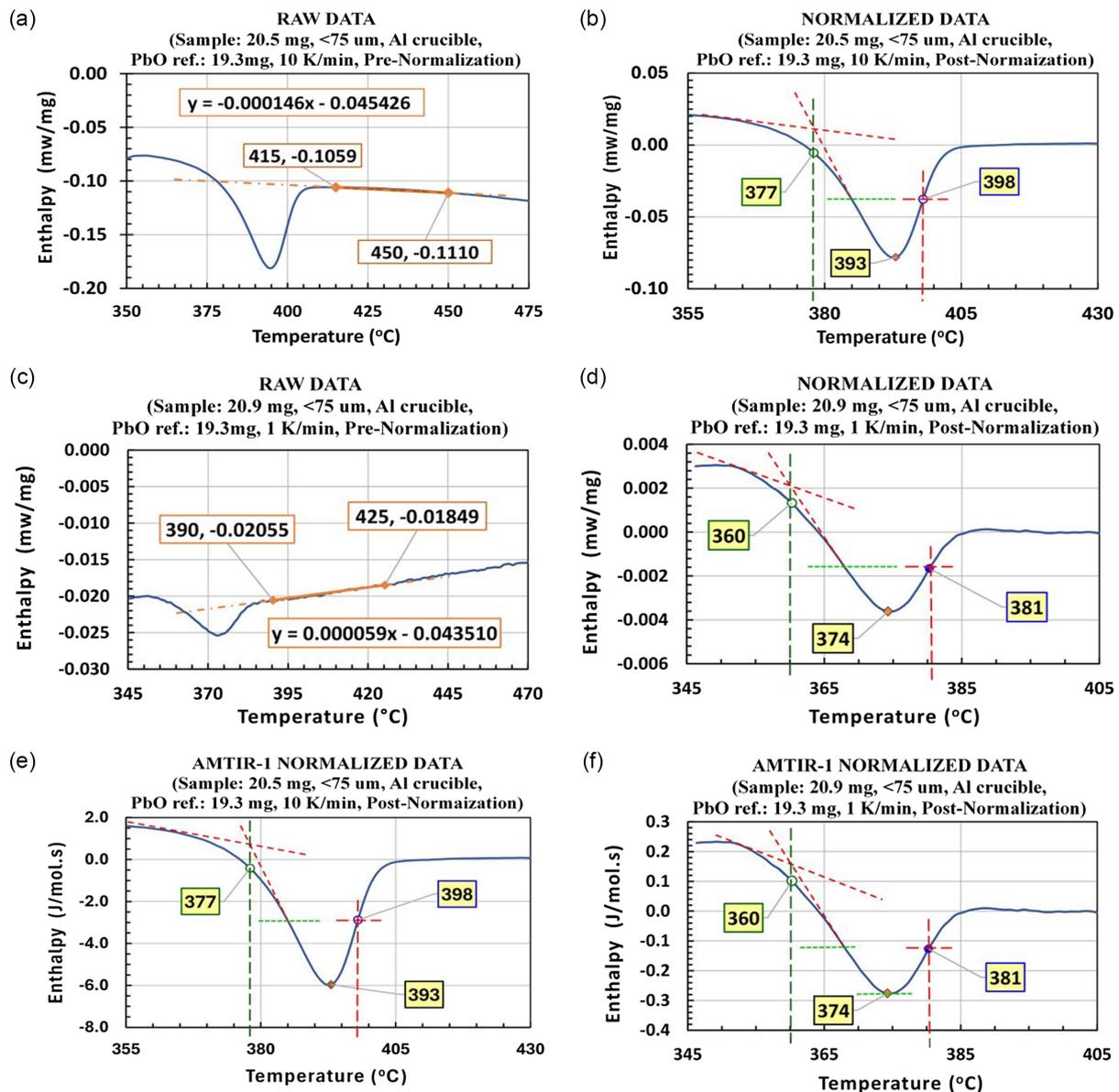
using this method. (Comparisons of our key point data values prior and post baseline correction demonstrated potential for measurement differences of greater than ±4.3 °C.)

Employing this approach on the 10 K/min thermogram experiment, the EXCEL built-in regression analyzer calculated a linear equation for this trendline, **y = −0.000146x − 0.045426**, (Figure 2(a)) where "**y**" is the value to be subtracted from the "raw" enthalpy column value at temperature "**x**" (*Increase the trendline "number" value to at least 6 digits.*). This new column was labeled as "Normalized (*or baseline corrected*) Enthalpy". Together with the Original Temperature value column, these data

points were used to create Figure 2(b), the 10 K/min DSC curve for AMTIR-1. As can be seen, the enthalpy found immediately after the primary endotherm has been brought to baseline level in terms of mw/mg.

Two key points have been identified from the new data. The first point is the *thermal event,* $\mathbf{T_g(\alpha)}$ historically misrepresented as the fundamental glass transition (T_g); the data point found at the intersection of the opposing first derivatives for the leading edge of the primary endotherm. For the 10 K/min analysis, this data point is identified as $\mathbf{T_g(10)}$; meaning that it is the "$\mathbf{T_g}$-*like*" thermal event measured at **10 K/min** and occurs at 377 °C. This

Figure 3
**(a) Normalized 10 K/min and 1 K/min AMTIR-1 DSC data, demonstrating enthalpy scale and endotherm
peak differences due solely to experimental heating rate. (b) ZHR analysis of 10 K/min and 1 K/min DSC data,
demonstrating solutions of key viscosity points for the isothermal equilibrium, true T_g and T_D extrapolated values and
demonstrating the equation constant "C" (*slope*) to be equal within the composition. (*Abscissa in Log scale*)**
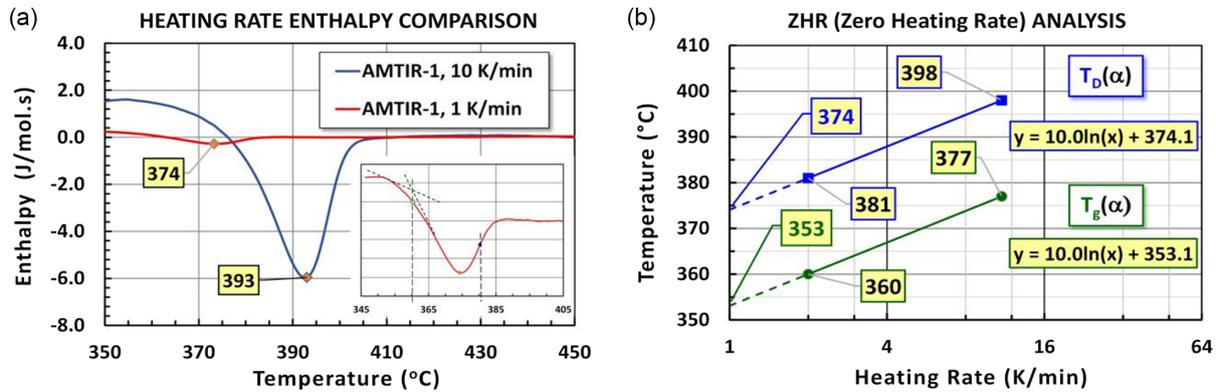
data point as well as all other Tg-related points is determined directly, using EXCEL and calculus algorithm techniques developed by the authors. It may also be determined manually. However, as the error can be excessive if only 2 heating rates are employed it is not recommended. The second key point is the 10 K/min DSC endotherm FWHM trailing edge temperature [**FWHMte(10)**]. It occurs at 398 °C. In similar fashion, this process is repeated for the data obtained by a **1 K/min** DSC experiment to create Figure 2(c) and (d). AMTIR-1 yielded a **$T_g(1)$** DSC value of 360 °C and a **FWHMte(1)** DSC value of 380 °C.

A DSC instrument yields enthalpy data in mw/mg (*power per unit of mass, P/m*), as a calculated field which makes use of sample mass (*in milligrams*) entered by the user into the device's input field. Since 1 mw/mg is equivalent to 1 w/g, and since 1 watt equals 1 J/s, then **1 P/m** is equal to 1 watt/g which is equal to **1 J/g.s**. The equivalent molecular weight, M_x^{eq} of a glass compound x, is defined as the number of grams of the glass compound x which equates to 1 mole (Avogadro's Number) of the compound's constituent atoms.

The equivalent molecular weight of a particular ChG, M_{ChG}^{eq}, may be calculated by summing the individual atomic percentages for each element in the ChG composition multiplied by their respective atomic weights. Therefore, multiplying a properly normalized DSC thermogram's enthalpy output data by the factor M_{ChG}^{eq} yields a thermogram with an ordinate axis in **J/mol.s**. For example, As_2Se_3 has 40% of the atoms in a mole of atoms that are As and 60% of the atoms in a mole of atoms that are Se. The $M_{As_2Se_3}^{eq}$ is 77.344 g/mol. P/m x M_x^{eq} for a particular glass compound is the conversion from J/g.s to J/mol.s.

Thus, $M_{AMTIR-1}^{eq}$ equals [(0.33x72.64) + (0.12x74.92) + (0.55x78.96)], or **76.39 g/mol**, a factor which is applied to the normalized output data of Figure 2(b) and (d) to produce Figure 2(e) and (f) in ordinate units of **J/mol.s**. This "power-correlated" presentation of the DSC data will be useful for those researchers interested in evaluating glass energy states as a function of time using time integration.

Figure 3(a) combines the two experiments (10 K/min and 1 K/min) in a manner which clearly illustrates the differences in the amplitudes of the enthalpy signals. Modern DSC instruments incorporate "autogain" technology, which optimizes thermal measurement sensitivity, based on initial sample response. However, both fast and small heating rates create their own analysis challenges. Small heating rates result in small enthalpy signal outputs, which may make visual observations and judgments more

difficult and subjective. High heating rates result in potential loss of data if the equipment is not yielding sufficient data per unit time. Therefore, two equipment setup considerations are important: (1) incorporate a minimum of 4 data points per temperature degree change and (2) maintain the calibration and performance of the instrument at all heating rates with known library standards.

The experimental temperature values measured (*evaluated by calculus or manual derivative techniques*) at 10 and 1 K/min (Table 2) were graphically extrapolated at a limiting heating rate of 0 K/min, a **ZHR** as shown in Figure 3(b). Per our equation-7, this is accomplished by adding the value "**1**" to each heating rate, as well as dividing the heating rate (**α**) by the value of (**$\alpha+1$**) to satisfy the requirement that logarithm arguments are unitless. [i.e., $1+(\alpha/\alpha_1)$) where $\alpha_1 = 1$ K/min]. Use EXCEL's log scale for the abscissa and plot this value against the corresponding "**α**" temperature value. The trendline values will then intercept with the $\alpha = 1$ abscissa. Since the logarithm of 1 is zero, we are mathematically at the ZHR value, for the isothermal, equilibrium T_g and FWHM te values.

Figure 3(b) presents the ZHR analysis. This new mathematical approach was developed by two of our team members and discussed in greater detail in references [3, 30]. Note that the constants "C" (*slopes*) for each of the two key viscosity point solutions within the composition are equal (*10.0 for AMTIR-1*). We have found this equality relationship between T_g and T_D to hold true for all ChGs studied to date. We conclude that within a glass composition, the slopes should be equal within experimental error for the key viscosity points if the data is analyzed correctly. We have found that absolute average values for C do seem to vary a small amount between ChG glass families. To date, we have only studied selenides, sulfides, and tellurides. We are in the process of gathering more data on this aspect of ZHR analysis. (*See* Table 3 *for more information.*)

Table 2
AMTIR-1 experimental DSC data used for ZHR analysis

(α) Rate	($\alpha+1$) Rate	[1+(α/α_1)] Rate	T_g	T_D
K/min	K/min	K/min	°C	°C
10	11	11	377	398
1	2	2	360	381
ZHR Analysis ("0 K/min" values)			**353**	**374**

Table 3
Summary of DSC and dilatometer data comparing key viscosity points

Chalcogenide glass		AMTIR-1		AMTIR-2		AMTIR-3		AMTIR-6		AMTIR-F1		18-UCF-6		UCF-512	
Measurement Parameters		DSC and CTE Dilatometer Thermogram Temperature Data, Data Point Locations, and Comparisons													
DSC and CTE Temperature Data ("T" values in °C)		$T_g(\alpha)$	$T_D(\alpha)^2$	$T_g(\alpha)$	$T_D(\alpha)$	$T_g(\alpha)$	$T_D(\alpha)$	$T_g(\alpha)$	$T_D(\alpha)$	$T_g(\alpha)$	$T_D(\alpha)$	$T_g(\alpha)$	$T_D(\alpha)$	$T_g(\alpha)$	$T_D(\alpha)$
$\alpha = 1$ K/min	T (1)	360	381	166	182	275	295	189	206	140	156	186	201	186	208
$\alpha = 10$ K/min	T (10)	**377**	398	**183**	199	**292**	312	**207**	224	**156**	172	**204**	216	**203**	223
ZHR Constant "C"	(°C)	10.0	10.0	10.0	10.0	10.0	10.0	10.6	10.6	9.4	9.4	10.1	10.0	10.0	10.1
DSC Thermogram	$T_g(0)$	353		158		268		182		134		179		180	
10:1 ZHR Analysis	$T_D(0)$		374		175		288		199		150		193		202
CTE Thermogram	T_g	353		159		268		182		133		179		181	
Derivative Values	T_D		374		175		290		200		151		195		202
Comparison ΔT_g	ΔT_D (°C)	0	0	−1	0	0	−2	0	−1	+1	−1	0	−2	−1	0

Figure 4
Coefficient of thermal expansion (Dilatometry) data for AMTIR-1 with key temperature and viscosity points identified. (*See Table 3 for usage*.)
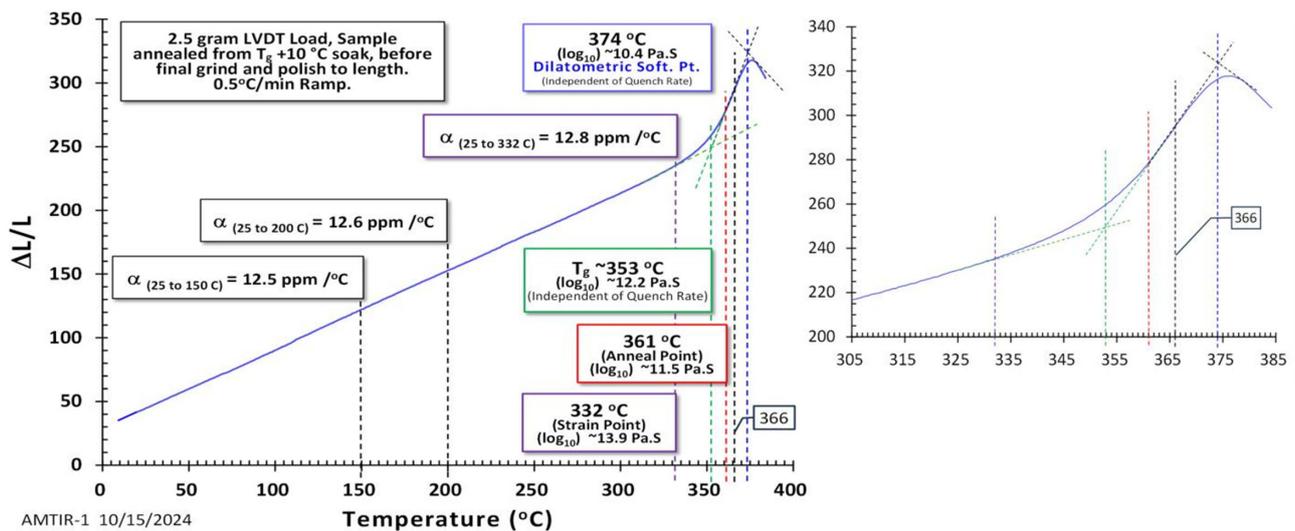
The T_g temperature value calculated by this technique was confirmed by performing an independent evaluation of the coefficient of thermal expansion (CTE) measurement of AMTIR-1, as shown in Figure 4. As seen, values are considerably smaller than their 10 K/min counterparts typically reported in scientific literature. (*Routinely employed and published 20 K/min heating rate-derived values would be higher and more inaccurate.*)

This table shows that isothermal equilibrium, glass transition temperatures determined by our new ZHR method consistently occur at temperatures where independently determined rheological profiles conducted by our labs and many other research facilities throughout the world assign viscosity values of $\log_{10}(\eta) = 12.2 \pm 0.2$ Pa.s. These data also support our contention that a previously unknown and/or unpublished relationship exists between the FWHM te of the primary endotherm and the dilatometric

softening point (T_D), a key point we measured using the same analytical tools and methods used to determine the T_g value. Our rheological studies on many ChGs assign viscosity values of $\log_{10}(\eta) = 10.4 \pm 0.2$ Pa.s to this key point.

4. Conclusions

Multiple commercial and lab-scale ChGs were evaluated using a new T_g measurement protocol with a conventional DSC, to show that the resolved value of the isothermal equilibrium Glass Transition Temperature, $T_g(0)$, now called a ZHR T_g, is effectively equal to the Glass Transition Temperature determined using an appropriate dilatometric measurement technique. Our precision dilatometry measurements *(i.e., near isothermal equilibrium measurements, at near-zero dilation sensor loads)* provide objective physical property temperature values for associated key viscosity points. The evaluation of the experimental data validates our theory and the method described accurately demonstrates the ability of the approach to define other thermogram properties. While applied here to ChGs, the authors

---

[2] $T_D(\alpha)$ **FWHM te** is the Full Width Half Maximum, "trailing edge" of the first DSC Endotherm, which we have associated in our work with the Dilatometric Softening Point (T_D), with a correlated viscosity value of $\log_{10}(\eta) \sim 10.4$ Pa.s and a molecular relaxation time constant on the order of one second.

believe that the experimental procedures and analytical approach described in this study can be employed universally with any glass system.

Illogical and incorrect mathematical relationships applied in the past have been replaced with models that can be applied with confidence. Moreover, the tools presented in this paper can be applied faithfully to future DSC thermogram research. A review of the majority of research publications on ChGs available to the public (*such as those referenced in this paper*) will show that $T_g(10)$ values are often advocated by followers of Moynihan and Kissinger and are incorrect. These solutions are typically 17 °C higher than $T_g(0)$ values and can be much higher, leading to physical property errors, product misrepresentations, and field application failures. Applying this study's precise methodologies and analytics, the significance of all previously published DSC values defined as "the glass transition" can now be accurately redefined as the appropriate $T_g(\alpha)$ values, where "α" is the heating rate (K/unit time).

It was shown that the DSC's first endotherm FWHM te(0) extrapolated values exist at temperatures which are identical or nearly identical to those of independent CTE-derived T_D values. We assign the term "T_D" to the DSC evaluated value. The time constant for molecular relaxation at the dilatometric softening point T_D is on the order of one second and the same time constant may now be assigned to DSC-derived T_D values. We present a revised interpretation of T_D (*or the limiting DSC FWHM te*) as the temperature at which a glass first clearly demonstrates irreversible deformation, resulting in rapid geometric morphing. In an upcoming publication, members of our team will provide enhanced theory on the glass transition, using DSC data to locate and to define the exact temperature associated with the "endpoint" of the isothermal equilibrium glass transition region using specific data from the first endotherm and ZHR. This new temperature (viscosity) point is different from T_D and occurs slightly before it.

The logical extension of this study is the production of a full "ZHR limit" thermogram for any ChG composition of interest. Such a thermogram will identify the true location of all endothermic and exothermic behavior, as well as deliver far more accurate and useful enthalpy data. It will yield more precise knowledge of susceptibility of nucleation and crystallization for phase change materials. Perhaps, more importantly, combining such data with our team member's corrected equations for the activation energy of crystallization [30] will greatly improve the outcome of any nucleation and crystallization experiments, such as those associated with GRIN glass production.

Funding Support

Acknowledgement

Ethical Statement

This study does not contain any studies with human or animal subjects performed by any of the authors.

Conflicts of Interest

The authors declare that they have no conflicts of interest to this work.

Data Availability Statement

Data are available from the corresponding author upon reasonable request.

Author Contribution Statement

Thomas J. Loretz: Conceptualization, Methodology, Software, Validation, Formal analysis, Data curation, Writing – original draft, Writing – review & editing, Visualization, Project administration. **Rashi Sharma:** Investigation, Resources, Writing – review & editing. **Anna Zachariou:** Investigation, Resources. **Richard A. Loretz:** Validation, Formal analysis, Data curation, Writing – review & editing, Visualization. **Myungkoo Kang:** Investigation, Writing – review & editing. **Kathleen A. Richardson:** Conceptualization, Validation, Writing – review & editing, Supervision, Project administration, Funding acquisition.

References

[1] Pye, L. D. (1972). The vitreous state. In L. D. Pye, H. J. Stevens & W. C. LaCourse (Eds.), *Introduction to glass science* (pp. 1–30). Springer. https://doi.org/10.1007/978-1-4757-0328-3_1

[2] Loretz, R. A., Loretz, T. J., & Richardson, K. A. (2022). Predictive method to assess chalcogenide glass properties: Bonding, density and the impact on glass properties. *Optical Materials Express*, *12*(5), 2012–2027. https://doi.org/10.1364/OME.455523

[3] Loretz, R. A., & Loretz, T. J. (2024). Corrections to theoretical glass transition temperature models and interpretations with application examples to chalcogenide glass. *Journal of Non-Crystalline Solids*, *628*, 122845. https://doi.org/10.1016/j.jnoncrysol.2024.122845

[4] Hagy, H. E. (1972). Rheological behavior of glass. In L. D. Pye, H. J. Stevens & W. C. LaCourse (Eds.), *Introduction to glass science* (pp. 343–371). Springer. https://doi.org/10.1007/978-1-4757-0328-3_11

[5] Berthier, L., & Biroli, G. (2011). Theoretical perspective on the glass transition and amorphous materials. *Reviews of Modern Physics*, *83*(2), 587–645. https://doi.org/10.1103/RevModPhys.83.587

[6] Chazot, M., Arias, C., Kang, M., Blanco, C., Kostogiannes, A., Cook, J., . . ., & Richardson, K. A. (2021). Investigation of ZnSe stability and dissolution behavior in As-S-Se chalcogenide glasses. *Journal of Non-Crystalline Solids*, *555*, 120619. https://doi.org/10.1016/j.jnoncrysol.2020.120619

[7] Ikeda, M., & Aniya, M. (2013). Understanding the Vogel–Fulcher–Tammann law in terms of the bond strength–coordination number fluctuation model. *Journal of Non-Crystalline Solids*, *371*, 53–57. https://doi.org/10.1016/j.jnoncrysol.2013.04.034

[8] Kumar, R., Sharma, P., & Rangra, V. S. (2012). Kinetic studies of bulk $Se_{92}Te_{8-x}Sn_x$ (x = 0, 1, 2, 3, 4 and 5) semiconducting glasses by DSC technique. *Journal of Thermal Analysis and Calorimetry*, *109*(1), 177–181. https://doi.org/10.1007/s10973-011-1661-z

[9] Rysava, N., Spasov, T., & Tichy, L. (1987). Isothermal DSC method for evaluation of the kinetics of crystallization in the Ge-Sb-S glassy system. *Journal of Thermal Analysis*, *32*, 1015–1021. https://doi.org/10.1007/BF01905157

[10] Vázquez, J., Cárdenas-Leal, J. L., González-Palma, R., García-G. Barreda, D., López-Alemany, P. L., & Villares, P. (2011). An

integral method to analyze the glass-crystal transformation kinetics by differential scanning calorimetry under non-isothermal regime. Application to the crystallization of the Ge 0.08 Sb 0.15 Se 0.77 chalcogenide glass. *Journal of Materials Science*, 46, 5267–5277. https://doi.org/10.1007/s10853-011-5465-0

[11] Hu, J., Sun, X., Agarwal, A. M., Viens, J. F., Kimerling, L. C., Petit, L., . . . , & Richardson, M. (2007). Studies on structural, electrical, and optical properties of Cu-doped As-Se-Te chalcogenide glasses. *Journal of Applied Physics*, 101(6), 63520-1–65320-7. https://doi.org/10.1063/1.2712162

[12] Abu-Sehly, A. A., El-Oyoun, M. A., & Elabbar, A. A. (2008). Study of the glass transition in amorphous Se by differential scanning calorimetry. *Thermochimica Acta*, 472(1–2), 25–30. https://doi.org/10.1016/j.tca.2008.03.007

[13] Wang, R. P., Zha, C. J., Rode, A. V., Madden, S. J., & Luther-Davies, B. (2007). Thermal characterization of Ge-As-Se glasses by differential scanning calorimetry. *Journal of Materials Science: Materials in Electronics*, 18, 419–422. https://doi.org/10.1007/s10854-007-9229-1

[14] Yang, G., Gueguen, Y., Sangleboeuf, J. C., Rouxel, T., Boussard-Plédel, C., Troles, J., . . . , & Bureau, B. (2013). Physical properties of the $Ge_xSe_{1−x}$ glasses in the $0<x< 0.42$ range in correlation with their structure. *Journal of Non-Crystalline Solids*, 377, 54–59. https://doi.org/10.1016/j.jnoncrysol.2013.01.049

[15] Moynihan, C. T., Lee, S. K., Tatsumisago, M., & Minami, T. (1996). Estimation of activation energies for structural relaxation and viscous flow from DTA and DSC experiments. *Thermochimica Acta*, 280, 153–162. https://doi.org/10.1016/0040-6031(95)02781-5

[16] Moynihan, C. T., Easteal, A. J., Wilder, J., & Tucker, J. (1974). Dependence of the glass transition temperature on heating and cooling rate. *The Journal of Physical Chemistry*, 78(26), 2673–2677. https://doi.org/10.1021/j100619a008

[17] Málek, J. (2023). Structural relaxation in chalcogenide glasses. *Journal of the American Ceramic Society*, 106(3), 1739–1747. https://doi.org/10.1111/jace.18864

[18] Lasocka, M. (1976). The effect of scanning rate on glass transition temperature of splat-cooled $Te_{85}Ge_{15}$. *Materials Science and Engineering*, 23(2–3), 173–177. https://doi.org/10.1016/0025-5416(76)90189-0

[19] Larmagnac, J. P., Grenet, J., & Michon, P. (1981). Glass transition temperature dependence on heating rate and on ageing for amorphous selenium films. *Journal of Non-Crystalline Solids*, 45(2), 157–168. https://doi.org/10.1016/0022-3093(81)90184-8

[20] Patel, A. T., & Pratap, A. (2012). Study of kinetics of glass transition of metallic glasses. *Journal of Thermal Analysis and Calorimetry*, 110(2), 567–571. https://doi.org/10.1007/s10973-012-2527-8

[21] Honcová, P., Včeláková, M., Svoboda, R., Sádovská, G., & Málek, J. (2024). Structural relaxation of Sb_2Se_{98} chalcogenide glass and its effect on following crystallization. *Ceramics International*. Advance online publication. https://doi.org/10.1016/j.ceramint.2024.02.124

[22] Svoboda, R., Málek, J., & Liška, M. (2019). Correlation between the structure and structural relaxation data for $(GeSe_2)_y$ $(Sb_2Se_3)_{1-y}$ glasses. *Journal of Non-Crystalline Solids*, 505, 162–169. https://doi.org/10.1016/j.jnoncrysol.2018.11.013

[23] Ozawa, T. (1971). Kinetics of non-isothermal crystallization. *Polymer*, 12(3), 150–158. https://doi.org/10.1016/0032-3861(71)90041-3

[24] Kissinger, H. E. (1957). Reaction kinetics in differential thermal analysis. *Analytical Chemistry*, 29(11), 1702–1706. https://doi.org/10.1021/ac60131a045

[25] Patial, B. S., Kumari, A., Thakur, N., & Tripathi, S. K. (2024). A thermo-physical study of In additive Se-Te chalcogenide glasses. *Bulletin of Materials Science*, 47(1), 41. https://doi.org/10.1007/s12034-023-03111-1

[26] Abdel-Rahim, M. A., Abdel-Latief, A. Y., Soltan, A. S., & El-Oyoun, M. A. (2002). Crystallization kinetics of overlapping phases in $Cu_6Ge_{14}Te_{80}$ chalcogenide glass. *Physica B: Condensed Matter*, 322(3–4), 252–261. https://doi.org/10.1016/S0921-4526(02)01190-0

[27] Kut'in, A. M., Shiryaev, V. S., Plekhovich, A. D., & Plekhovich, S. D. (2020). Calorimetric and volumetric functions of As_xSe_{1-x} (x = 0.3–0.5) glasses and their model representation. *Journal of Thermal Analysis and Calorimetry*, 139, 1443–1452. https://doi.org/10.1007/s10973-019-08491-3

[28] Shpotyuk, M., & Shpotyuk, O. (2021). On the glass-transition temperature Tg in chalcogenide glass-forming systems: Critical assessment on compositional changes within covalent bond approach. *Physica B: Condensed Matter*, 603, 412720. https://doi.org/10.1016/j.physb.2020.412720

[29] Shpotyuk, M., Szlęzak, J., Shpotyuk, Y., Boussard-Pledel, C., Bureau, B., Balitska, V., . . . , & Shpotyuk, O. (2020). On the glass transition temperature T_g against molar volume V_m plotting in arsenoselenide glasses. *Journal of Non-Crystalline Solids*, 528, 119758. https://doi.org/10.1016/j.jnoncrysol.2019.119758

[30] Loretz, R. A., & Loretz, T. J. (2024). Modified chalcogenide glass equations for the activation energy of crystallization. *Journal of Optics and Photonics Research*, 1(1), 16–22. https://doi.org/10.47852/bonviewJOPR42022177

[31] Raoux, S. (2009). Phase change materials. *Annual Review of Materials Research*, 39(1), 25–48. https://doi.org/10.1146/annurev-matsci-082908-145405

[32] Dahshan, A. (2016). Crystallization kinetics of new $Ge_{20}Se_{60}Sb_{20-x}Ag_x$ (0≤x≤20 at.%) glasses. *Journal of Alloys and Compounds*, 670, 306–311. https://doi.org/10.1016/j.jallcom.2016.02.045

[33] Mahmoud, A. Z., Mohamed, M., Moustafa, S., Abdelraheem, A. M., & Abdel-Rahim, M. A. (2018). Study of non-isothermal crystallization kinetics of $Ge_{20}Se_{70}Sn_{10}$ chalcogenide glass. *Journal of Thermal Analysis and Calorimetry*, 131, 2433–2442. https://doi.org/10.1007/s10973-017-6793-3

[34] Kissinger, H. E. (1956). Variation of peak temperature with heating rate in differential thermal analysis. *Journal of Research of the National Bureau of Standards*, 57(4), 217–221. http://dx.doi.org/10.6028/jres.057.026

[35] Lafi, O. A. (2016). What are the parameters that glass transition temperature of chalcogenide glasses depend on? An overview. *Journal of Non-Oxide Glasses*, 8(1), 11–15.

[36] Hilton, A. R. Sr. (2010). *Chalcogenide glasses for infrared optics*. Dubuque, Iowa, USA: The McGraw Hill Companies. ISBN 978-0-07-159697-8. https://www.accessengineeringlibrary.com/content/book/9780071596978